HOKKAIDO UNIVERSITY

Title	Comparison between theory and experiment of nonlinear propagation for a-few-cycle and ultrabroadband optical pulses in a fused-silica fiber
Author(s)	Karasawa, Naoki; Nakamura, Shinki; Nakagawa, Naoya et al.
Citation	IEEE Journal of Quantum Electronics, 37(3), 398-404 https://doi.org/10.1109/3.910449
Issue Date	2001-03
Doc URL	https://hdl.handle.net/2115/45330
Rights	© 2001 IEEE. Personal use of this material is permitted. However, permission to reprint/republish this material for advertising or promotional purposes or for creating new collective works for resale or redistribution to servers or lists, or to reuse any copyrighted component of this work in other works must be obtained from the IEEE.
Type	journal article
File Information	JQE37-3_398-404.pdf



Hokkaido University Collection of Scholarly and Academic Papers : HUSCAP

Comparison Between Theory and Experiment of Nonlinear Propagation for A-Few-Cycle and Ultrabroadband Optical Pulses in a Fused-Silica Fiber

Naoki Karasawa, Shinki Nakamura, Naoya Nakagawa, Masato Shibata, Ryuji Morita, Hidemi Shigekawa, and Mikio Yamashita

***Abstract*—Wave-propagation equations, including effectively the second derivative in time under the condition of a small difference between the group and phase velocities and the first derivative in position ξ in the group velocity coordinate, are derived based on the slowly evolving wave approximation. These can describe ultrabroadband optical pulse propagation with not only self-phase modulation (SPM), but also induced-phase modulation (IPM) in the monocycle regime in a fiber. It is shown that linear dispersion effects can be rigorously included in the numerical calculations. Calculations including SPM in a single-mode fused-silica fiber with the Raman effect are performed and compared with experimental results. Also, calculations including IPM in the fused-silica fiber are compared with experimental results. The effects of each term in the calculations on spectra are analyzed and it is shown that inclusion of the Raman effect and the dispersion of the effective core area is important for obtaining better agreement with experiments. It is shown that inclusion of more than third-order dispersion terms is necessary for calculations of monocycle pulse propagation.**

***Index Terms*—Nonlinear fiber optics, ultrabroadband and monocycle pulse propagation, self- and induced-phase modulation.**

I. Introduction

THE RECENT development of ultrashort pulse lasers, as well as spectral-broadening and pulse-compression techniques, permit us to use optical pulses which have a duration as short as a few optical cycles with a bandwidth of several hundred terahertz. To describe the propagation of these pulses in a nonlinear optical medium, care must be taken to select what approximations may be used. The slowly varying envelope approximation (SVEA) has been used widely to describe nonlinear pulse propagation in an optical fiber [1]. However, it is applicable only to pulses whose temporal envelope changes slowly as compared with an optical cycle. The other issue is how to describe correctly the linear dispersion relations when the bandwidth of the pulse becomes large such that the conventional Taylor expansion at the center frequency and the use of only the first several terms may not be applicable. For a fused-silica optical fiber, up to the third-order terms are included conventionally [1]. It is straightforward to include higher order terms; however, it is not clear how many terms are required. For some cases, the dispersion relation is given such that the convergence of its Taylor series expansion is slow. For example, the loss dispersion of the capillary fiber is roughly proportional to $1/\omega^2$, where ω is the angular frequency [2]. Here, we show a method to rigorously include these linear dispersion relations.

Recently, we have proposed to use both induced-phase modulation (IPM) and self-phase modulation (SPM) to generate ultrabroadband optical pulses using a single-mode fused-silica fiber [3]–[5] and a capillary fiber filled with noble gas [6], [7]. For the fused-silica fiber, the Raman effect may become important when the pulse duration is close to the Raman response time [8], [9]. Here, equations including these effects are also presented.

To check the validity of the equations thus derived, we calculate spectrum broadening using single-mode fused-silica fiber. In addition, to evaluate the effect of newly added terms in the equation, calculations without one of these terms are also performed. The calculated spectra thus obtained are compared with the experimental spectra and the effect of each term is evaluated from this comparison.

In a recent paper, Brabec and Krausz theoretically showed [10] that the electric field envelope can describe an optical pulse whose duration is as short as one optical cycle and they derived an equation which they called the slowly evolving wave approximation (SEWA). Unlike their equations, ours include the Raman effect, IPM, and all order of terms for waveguide and material linear dispersion. Equations including the Raman effect for SPM are derived by Blow and Wood [11] and Mamyshev and Chernikov [12], where the dispersion of linear terms is included up to the fourth-order terms for [11] and up to the third-order terms for [12]. However, no explicit method for including all orders of linear dispersion terms was shown and no comparisons between calculated and experimental results for a few cycle pulses were performed.

Detailed comparisons between theoretical and experimental spectra have been done recently by Boyer [13] using ~100-fs

Manuscript received July 31, 2000; revised October 31, 2000.

N. Karasawa was with the Department of Applied Physics, Hokkaido University, Sapporo 060-8628, Japan, and also with CREST, Japan Science and Technology Corporation (JST), Sapporo 060-8628, Japan. He is now with the Chitose Institute of Science and Technology, Chitose 066-8655, Japan.

S. Nakamura was with the Department of Applied Physics, Hokkaido University, Sapporo 060-8628, Japan, and also with CREST, Japan Science and Technology Corporation (JST), Sapporo 060-8628, Japan. He is now with the Department of Media and Telecommunications Engineering, Ibaraki University, Hitachi 316-8511, Japan.

N. Nakagawa, M. Shibata, R. Morita, and M. Yamashita are with the Department of Applied Physics, Hokkaido University, Sapporo 060-8628, Japan, and also with CREST, Japan Science and Technology Corporation (JST), Sapporo 060-8628, Japan.

H. Shigekawa is with the Institute of Materials Science, University of Tsukuba, Tsukuba 305-8573, Japan, and also with CREST, Japan Science and Technology Corporation (JST), Tsukuba 305-8573, Japan.

Publisher Item Identifier S 0018-9197(01)01629-3.

0018–9197/01$10.00 © 2001 IEEE

pulses near the zero-dispersion wavelength, and the effects of the Raman, as well as the steepening terms, on spectra have been elucidated.

II. Nonlinear Optical Pulse Propagation Equations

We start from the Maxwell equation and its Fourier transform

$$\nabla^2\mathbf{E}(x,y,z,t) - \frac{1}{c^2}\partial_t^2\mathbf{D_L}(x,y,z,t) = \mu_0\partial_t^2\mathbf{P_{NL}}(x,y,z,t), \tag{1}$$

$$\left(\nabla_\perp^2 + \partial_z^2 + \frac{\varepsilon(\omega)\omega^2}{c^2}\right)\tilde{\mathbf{E}}(x,y,z,\omega) = -\mu_0\omega^2\tilde{\mathbf{P}}_{\mathbf{NL}}(x,y,z,\omega) \tag{2}$$

where

$\mathbf{E}$	electric field;
$\mathbf{D_L}$	linear electric displacement;
$\mathbf{P_{NL}}$	nonlinear polarization;
c	speed of light;
μ_0	vacuum permeability;
$\varepsilon(\omega)$	linear dielectric constant;
ω	angular frequency;
$\nabla_\perp^2$	$= \partial_x^2 + \partial_y^2$;

and the Fourier transform is defined as $\tilde{\mathbf{E}}(x,y,z,\omega) = \int_{-\infty}^{\infty}\mathbf{E}(x,y,z,t)\exp(i\omega t)\,dt$. We consider propagation to be in the z direction and assume that all fields are polarized in the x direction and, hence, consider only that component. Then we write $\mathbf{E}(x,y,z,t) = \hat{\mathbf{x}}[E(x,y,z,t)\exp(-i\omega_0 t) + \text{c.c.}]/2$, where $\hat{\mathbf{x}}$ is the unit vector in the x direction, ω_0 is the center angular frequency, and *c.c.* specifies the complex conjugate. We also assume that the Fourier transform of the electric field $E(x,y,z,t)$ and the nonlinear polarization envelope functions can be written in the following form:

$$\tilde{E}(x,y,z,\omega) = F(x,y,\omega)\tilde{A}(z,\omega-\omega_0)\exp(i\beta_0 z) \tag{3}$$

$$\tilde{P}_{\text{NL}}(x,y,z,\omega) = \varepsilon_0\chi^{(3)}(\omega)F^3(x,y,\omega)\tilde{p}_{\text{NL}}(z,\omega-\omega_0)\times\exp(i\beta_0 z) \tag{4}$$

where ε_0 is the vacuum dielectric constant, and $\beta_0 \equiv \beta(\omega_0)$ is the real part of the propagation constant at ω_0. Here, we consider only the third-order nonlinear optical effect with the coefficient $\chi^{(3)}(\omega)$. We assume that we can separate the forward-propagating wave and the backward-propagating wave and consider only the one propagating forward. Using first-order perturbation theory [1] in (2), we obtain

$$\left(\partial_z^2 + 2i\beta_0\partial_z - \beta_0^2 + \gamma^2(\omega)\right)\tilde{A}(z,\omega-\omega_0) = -\frac{\omega^2 N(\omega)\chi^{(3)}(\omega)}{c^2}\tilde{p}_{\text{NL}}(z,\omega-\omega_0) \tag{5}$$

where $\gamma(\omega) \equiv \beta(\omega) + i\alpha(\omega)/2$ is the propagation constant without the nonlinear terms and is determined by the unperturbed cross-section field equation $(\nabla_\perp^2 + \varepsilon(\omega)\omega^2/c^2)F(x,y,\omega) = \gamma^2(\omega)F(x,y,\omega)$. Also, $N(\omega) = \int F^4(x,y,\omega)\,dx\,dy/\int F^2(x,y,\omega)dx\,dy$. Thus, $\gamma(\omega)$ contains both material dispersion and waveguide dispersion. $\gamma(\omega)$ can have an imaginary part even if the material does not have a loss or gain as in the case of propagation in a capillary fiber [2]. Converting the units of A to [watt$^{1/2}$] by multiplying $(\int F^2(x,y,\omega)dxdy)^{1/2}/(2/\varepsilon_0 cn(\omega))^{1/2}$ and using the relations $\chi^{(3)}(\omega) = 8n(\omega)n_2(\omega)/3$ and $n_2^I(\omega) = 2n_2(\omega)/\varepsilon_0 cn(\omega)$, where n is the linear index of refraction of the medium, we have

$$\left(\partial_z^2 + 2i\beta_0\partial_z - \beta_0^2 + \gamma^2(\omega)\right)\tilde{A}(z,\omega-\omega_0) = -\frac{8n(\omega)n_2^I(\omega)\omega^2}{3c^2A_{\text{eff}}(\omega)}\tilde{p}_{\text{NL}}(z,\omega-\omega_0) \tag{6}$$

where

$$A_{\text{eff}}(\omega) = \frac{\left(\int F^2(x,y,\omega)dx\,dy\right)^2}{\int F^4(x,y,\omega)dx\,dy}. \tag{7}$$

Taking the inverse Fourier transform of (6), we have

$$\left(\partial_z^2 + 2i\beta_0\partial_z - \beta_0^2 + \hat{D}^2\right)A(z,t) = -\frac{8g(\omega_0)\omega_0^2}{3c^2}\left(1+\frac{i}{\omega_0}\partial_t\right)^2 \times (1 + i(\partial_\omega(\ln g(\omega))|_{\omega_0})\partial_t)p_{\text{NL}}(z,t) \tag{8}$$

where $g(\omega) = n(\omega)n_2^I(\omega)/A_{\text{eff}}(\omega)$, and we include the dispersion of $g(\omega)$ up to the first-order terms in the Taylor expansion at ω_0. $\hat{D}$ is given by the Taylor expansion of the propagation constant as

$$\hat{D} = \sum_{n=0}^{\infty}\frac{i^n}{n!}\left(\partial_\omega^n\left(\beta(\omega) + \frac{i\alpha(\omega)}{2}\right)\Big|_{\omega_0}\right)\partial_t^n. \tag{9}$$

At this point, we convert the time coordinate such that the pulse center is always at the time origin as $T = t - \dot{\beta}_0 z$ ($\dot{\beta}_0 = \partial_\omega(\beta(\omega))|_{\omega_0}$) and $\xi = z$ ($\partial_t = \partial_T, \partial_z = \partial_\xi - \dot{\beta}_0\partial_T$). Then we have

$$\left[\partial_\xi^2 + 2i\beta_0\left(1 + i\frac{\dot{\beta}_0}{\beta_0}\partial_T\right)(\partial_\xi - i\hat{D}') + \hat{D}'^2\right]A(\xi,T) = -\frac{8g(\omega_0)\omega_0^2}{3c^2}\left(1+\frac{i}{\omega_0}\partial_T\right)^2 \times (1 + i(\partial_\omega(\ln g(\omega))|_{\omega_0})\partial_T)p_{\text{NL}}(\xi,T) \tag{10}$$

where $\hat{D}' = \hat{D} - \beta_0 - i\dot{\beta}_0\partial_T$. Applying the operator $(2i\beta_0(1 + i\dot{\beta}_0\partial_T/\beta_0))^{-1}$ to both sides of this equation, we have

$$\left[\frac{1}{2i\beta_0}\left(1 + i\frac{\dot{\beta}_0}{\beta_0}\partial_T\right)^{-1}\left(\partial_\xi^2 + \hat{D}'^2\right) + \partial_\xi - i\hat{D}'\right]A(\xi,T) = i\frac{4g(\omega_0)\omega_0^2}{3c^2\beta_0}\left(1 + i\frac{\dot{\beta}_0}{\beta_0}\partial_T\right)^{-1}\left(1+\frac{i}{\omega_0}\partial_T\right)^2 \times (1 + i(\partial_\omega(\ln g(\omega))|_{\omega_0})\partial_T)p_{\text{NL}}(\xi,T). \tag{11}$$

The first term on the left hand side of this equation can be ignored if $|\partial_\xi A| \ll \beta_0|A|$, which physically means that the spatial

variation of the envelope is much slower than the wavelength. Also, we can show that

$$\left(1+i\frac{\dot{\beta}_0}{\beta_0}\partial_T\right)^{-1}\left(1+\frac{i}{\omega_0}\partial_T\right)^2 = 1+i\left(\frac{2}{\omega_0}-\frac{\dot{\beta}_0}{\beta_0}\right)\partial_T-\left(\frac{\dot{\beta}_0}{\beta_0}-\frac{1}{\omega_0}\right)^2 \times\partial_T^2\left(1+i\frac{\dot{\beta}_0}{\beta_0}\partial_T\right)^{-1}.$$

The third term on the right hand side of the above equation can be neglected if the difference between the group velocity ($v_g = 1/\dot{\beta}_0$) and the phase velocity ($v_p = \omega_0/\beta_0$) of the pulse is small. These two approximations are the same as the SEWA in [10], but unlike SVEA, and in these approximations there are no conditions specifying the slowness of the temporal change of the envelope as compared with the optical cycle time. Thus, this equation can be used for pulses as short as a single optical cycle. By using these approximations, (10) becomes

$$\partial_\xi A(\xi,T) = i(\hat{D}'+\hat{D}_{\rm corr})A(\xi,T) + i\frac{4g(\omega_0)\omega_0^2}{3c^2\beta_0}(1+is\partial_T)p_{\rm NL}(\xi,T) \quad (12)$$

where $\hat{D}_{\rm corr} = (1+i\dot{\beta}_0\partial_T/\beta_0)^{-1}\hat{D}'^2/2\beta_0$ and $s = 2/\omega_0 - \dot{\beta}_0/\beta_0 + \partial_\omega(\ln g(\omega))|_{\omega_0}$.

III. Nonlinear Terms

The nonlinear term $p_{\rm NL}$ may contain both the instantaneous Kerr nonlinearity as well as the delayed Raman response. Considering only the forward-propagating wave, it can be written as

$$p_{\rm NL}(\xi,T) = \frac{1}{4}\int_0^\infty R(T')[2|A(\xi,T-T')|^2A(\xi,T) + A^2(\xi,T-T')A^*(\xi,T)\exp(2i\omega_0T')]\,dT' \quad (13)$$

where the response function $R(t)$ is given by

$$R(T) = (1-f_R)\delta(T)+f_Rh_R(T). \quad (14)$$

For fused-silica, $f_R = 0.3$ and

$$h_R(T) = \frac{\tau_1^2+\tau_2^2}{\tau_1\tau_2^2}\exp(-T/\tau_2)\sin(T/\tau_1) \quad (15)$$

where $\tau_1 = 12.2$ fs and $\tau_2 = 32$ fs [11]. Since changes in h_R are much slower than an optical cycle at $2\omega_0$, (13) can be written as

$$p_{\rm NL}(\xi,T) = \frac{3}{4}[(1-f_R)|A(\xi,T-T')|^2 + \frac{2}{3}f_R\int_0^\infty h_R(T')|A(\xi,T-T')|^2\,dT']A(\xi,T). \quad (16)$$

IV. Equations for IPM

If two pulses are co-propagating in the same medium, we have IPM, as well as SPM. For each pulse j ($j = 1$ or 2), we obtain the following equation:

$$\partial_{\xi_j}A_j(\xi_j,T_j) = i(\hat{D}'_j+\hat{D}_{{\rm corr},j})A_j(\xi_j,T_j) + i\eta_j\left[(1+is_j\partial_{T_j})S_j+\frac{h_j(\omega_{0j})}{g(\omega_{0j})}(1+iu_j\partial_{Tj})I_j\right] \quad (17)$$

where

$$S_j = [(1-f_R)|A_j(\xi_j,T_j)|^2 + \frac{2}{3}f_R\int_0^\infty h_R(T')|A_j(\xi_j,T_j-T')|^2dT']A_j(\xi_j,T_j)$$

$$I_j = [2(1-f_R)|A_{3-j}(\xi_{3-j},T_{3-j})|^2 + \frac{2}{3}f_R\int_0^\infty h_R(T')|A_{3-j}(\xi_{3-j},T_{3-j}-T')|^2dT'] \cdot A_j(\xi_j,T_j).$$

In this equation, $\eta_j = \omega_{0j}^2g(\omega_{0j})/c^2\beta_{0j}, \xi_j = z$, and $T_j = t-\dot{\beta}_{0j}z$. $\hat{D}'_j, \hat{D}_{\rm corr,j}$ and s_j are obtained from $\hat{D}', \hat{D}_{\rm corr}$ and s by replacing ω_0 and $\partial_\omega^n(\gamma(\omega))|_{\omega_0}$ with ω_{0j} and $\partial_\omega^n(\gamma(\omega))|_{\omega_{0j}}$, respectively. Also, $h_j(\omega) = n(\omega)n_2^I(\omega)/O(\omega,\omega_{03-j}), u_j = 2/\omega_{0j}-\dot{\beta}_{0j}/\beta_{0j}+\partial{\rm In}(h_j(\omega))|_{\omega 0j}$, and

$$O(\omega,\omega_{03-j}) = \frac{\int F^2(x,y,\omega)dxdy\int F^2(x,y,\omega_{03-j})dxdy}{\int F^2(x,y,\omega)F^2(x,y,\omega_{03-j})dxdy.}$$

These terms appear because of the difference of the overlap of the spatial modes for induced phase modulation.

V. Numerical Calculations

Equations (12) or (17) can be calculated by the split-step Fourier method [1] where dispersion terms are calculated in the frequency domain and the nonlinear terms are calculated in the time domain. Dispersion terms can be evaluated in the frequency domain as

$$\hat{D}'(\omega) = \beta(\omega)+\frac{i\alpha(\omega)}{2}-\beta_0-\dot{\beta}_0(\omega-\omega_0) \quad (18)$$

$$\hat{D}_{\rm corr}(\omega) = \frac{\hat{D}'^2(\omega)}{2(\beta_0+\dot{\beta}_0(\omega-\omega_0))}. \quad (19)$$

In the numerical calculations, we utilize the Sellmeier equation to model the dispersion relation of the fused-silica fiber [14], where the refractive index $n(\lambda)$ of the fused-silica as a function of wavelength λ in μm ($0.21\ \mu{\rm m} < \lambda < 3.71\ \mu{\rm m}$) is given as

$$n^2(\lambda)-1 = \frac{0.696\,166\,3\lambda^2}{\lambda^2-(0.068\,404\,3)^2}+\frac{0.407\,942\,6\lambda^2}{\lambda^2-(0.116\,241\,4)^2} + \frac{0.897\,479\,4\lambda^2}{\lambda^2-(9.896\,161)^2}.$$

The propagation constant and its derivatives can be calculated from this equation for any ω. In practice, only the limited number of frequency points used in the fast Fourier transform routine are used in calculations and (18) and (19) are evaluated once and stored in the memory. Thus, the calculation of this method is very efficient.

VI. Comparison With the Previous Derivation

A. The SVEA Equation

In the SVEA, we neglect the ∂_z^2 term in (6). Also, it is assumed that $\gamma^2(\omega)-\beta_0^2 = 2\beta_0(\gamma(\omega)-\beta_0)$ in (6) [1]. After these operations and dividing both sides of this equation by $2i\beta_0$, we obtain

$$(\partial_z - i(\gamma(\omega)-\beta_0))\tilde{A}(z,\omega-\omega_0) = i\frac{4n(\omega)n_2^I(\omega)\omega^2}{3c^2A_{\text{eff}}(\omega)\beta_0}\tilde{p}_{\text{NL}}(z,\omega-\omega_0). \tag{20}$$

By taking the inverse Fourier transform of this equation, neglecting terms containing powers of ∂_t/ω_0 from the assumption $|\partial_t A/\omega_0| \ll |A|$, converting to the moving time coordinate ($T = t - \dot{\beta}_0 z$), and approximating $\hat{D}' \simeq -\beta_0^{(2)}\partial_T^2/2 - i\beta_0^{(3)}\partial_T^3/6$ for the fused-silica fiber ($\beta_0^{(j)} = \partial_\omega^j(\beta(\omega))|_{\omega_0}$), we have

$$\partial_\xi A(\xi,T) = \left(-\frac{i}{2}\beta_0^{(2)}\partial_T^2 + \frac{1}{6}\beta_0^{(3)}\partial_T^3\right)A(\xi,T) + i\frac{4g(\omega_0)\omega_0^2}{3c^2\beta_0}p_{\text{NL}}(\xi,T). \tag{21}$$

In addition to the assumptions $|\partial_\xi A| \ll \beta_0|A|$ and $|\partial_T A| \ll \omega_0|A|$, $|\gamma(\omega)-\beta_0| \ll |\beta_0|$ is conventionally assumed in the SVEA. The latter condition implies that $|\omega-\omega_0| \ll |\omega_0|$ for the fused-silica fiber and this condition is clearly not satisfied for the experimental situations considered here. Also in the conventional SVEA, the Raman term is not considered in $\mathbf{P_{NL}}$ ($f_R = 0$ in (16) and (17)).

B. The Equation by Blow and Wood

In the paper by Blow and Wood [11], the right hand side of (6) is formally defined as $-\hat{\Pi}\tilde{A}$ using the operator $\hat{\Pi}$ and is written as

$$(i\partial_z - \beta_0 + \sqrt{\gamma^2(\omega)+\hat{\Pi}}) \times (i\partial_z - \beta_0 - \sqrt{\gamma^2(\omega)+\hat{\Pi}})\tilde{A} = 0. \tag{22}$$

It is identified that the first term corresponds to the forward propagating wave and only the following equation is considered:

$$(i\partial_z - \beta_0 + \sqrt{\gamma^2(\omega)+\hat{\Pi}})\tilde{A} = 0. \tag{23}$$

By approximating $\sqrt{\gamma^2(\omega)+\hat{\Pi}} \simeq \gamma(\omega)+\hat{\Pi}/(2\gamma(\omega))$, we have

$$(\partial_z - i(\gamma(\omega)-\beta_0))\tilde{A} = \frac{i\hat{\Pi}\tilde{A}}{2\gamma(\omega)} = \frac{i4n(\omega)n_2^I(\omega)\omega^2}{3\gamma(\omega)c^2A_{\text{eff}}}p_{\tilde{\text{NL}}}. \tag{24}$$

For the fused-silica fiber case, we can set $\gamma(\omega) = \omega n(\omega)/c$. The inverse Fourier transformation and the conversion of the time coordinate yield

$$\partial_\xi A(\xi,T) = i\hat{D}'A(\xi,T) + i\frac{4g'(\omega_0)\omega_0}{3c} \times (1+is'\partial_T)p_{\text{NL}}(\xi,T) \tag{25}$$

where $g'(\omega_0) = n_2^I(\omega_0)/A_{\text{eff}}(\omega_0)$ and $s' = 1/\omega_0 + \partial_\omega(\ln g'(\omega))|_{\omega_0}$. This equation does not assume either $|\partial_z A| \ll \beta_0|A|$ or $|\partial_T A| \ll \omega_0|A|$. However, the nonlinear term must be small to satisfy $\sqrt{\gamma^2(\omega)+\hat{\Pi}} \simeq \gamma(\omega) + \hat{\Pi}/(2\gamma(\omega))$. In fact, for the present experimental situation, the condition $|\hat{\Pi}/\gamma^2(\omega)| \ll 1$ does not hold. However, its form is almost identical to the equation derived using the SEWA.

VII. Calculations for the Fused-Silica Fiber

A. 4.5-Cycle Pulse SPM Case

Calculations for 4.5-cycle pulses in a single-mode fused-silica fiber were performed and compared with experiment. In the experiments, pulses from a Ti:Sapphire oscillator (Femtolasers, M-1) were introduced to a 2.5-mm-long single-mode fiber (Newport F-SPV, the core radius $a = 1.32$ μm) by using a reflective objective. The pulse width measured by an autocorrelator was 12 fs and the input-pulse peak power calculated from the measured pulse energy at the fiber output was 175 kW. The input pulse was obtained by calculating the inverse Fourier transform of the spectrum of the input pulse. However, the transform-limited pulse width (8.6 fs) was smaller than the experimentally measured pulse width (12 fs) obtained by a fringe-resolved autocorrelator. To use the pulse with the correct spectrum and the pulse width in the calculation, the temporal duration was adjusted by adding quadratic spectral phase of the form $\phi(\omega) = c(\omega-\omega_0)^2$ to the experimental spectrum to make the inverse Fourier transform pulse width the same as that of the measured one. It gave the value $c = \pm 9.9$ fs^2/rad. Both values were used as initial calculations. However, it was found that the difference in the spectra was negligible. Thus, in the following, only the results with the negative value are shown.

We consider the material dispersion of fused-silica using the Sellmeier equation for the linear dispersion terms with zero loss. For single-mode fused-silica fiber, it is well known that the effective core area depends on the wavelength and it becomes larger as the wavelength becomes longer compared with the cutoff wavelength of the fiber [1]. For the fiber used in this experiment, the cut-off wavelength and the numerical aperture are 550 nm and 1.6, respectively, which give the core radius as 1.32 μm. It is estimated that at the long wavelength, the effective core area becomes quite large. For example, the effective core area A_{eff} calculated from the approximate fundamental mode distribution in [1] ($F = J_0(\kappa r)$ $(r < a)$ and $F = (a/r)^{1/2}J_0(\kappa a)e^{-\eta(r-a)}$ $(r > a)$, where $r = (x^2+y^2)^{1/2}, \kappa^2 = n_1^2k_0^2 - \beta^2$ and $\eta^2 = \beta^2 - n_2^2k_0^2, n_1$ and n_2 are refractive indices of the core and the clad, respectively) are $2.01\pi a^2$ at a wavelength of 790 nm and $3.68\pi a^2$ at 1000 nm, respectively. Thus, it is expected that, at longer wavelength, the

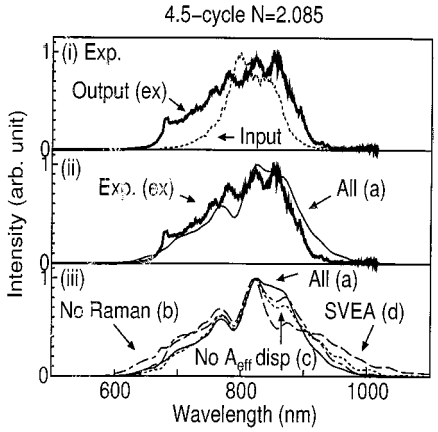


Fig. 1. The experimental and calculated spectra for 4.5-cycle pulse propagation in a 2.5-mm-long fused-silica fiber. The input power is 175 kW (soliton number $N = 2.085$). (i) Experimental input (thick solid line) and output (dotted line) spectra. (ii) Experimental spectrum (thick solid line) is compared with the calculated spectrum including all terms (solid line). (iii) Calculated spectra: (a) including all terms (solid line); (b) without the Raman term (dotted-dashed line); (c) without the effective core area dispersion (dotted line); and (d) the SVEA (dashed line).

nonlinear effect becomes smaller since the effective core area becomes larger. To include this effect in the calculation, the term $\partial_\omega(\ln g(\omega))|_{\omega_0}$ in (12) was calculated at the center wavelength and added for the steepening parameters. From the mode equation of the single-mode fiber, the derivative of the effective core area was numerically calculated as a function of wavelength and the value at center wavelength (798 nm) was obtained as $-\omega_0\partial_\omega(\ln A_{\text{eff}}(\omega))|_{\omega_0} = 2.06$. We used the value of the nonlinear refractive coefficient $n_2^I = 2.48\times10^{-20}$ m^2/W from [15].

Calculations with different levels of approximations were performed. For case (a), the Raman term as well as rigorous linear dispersion terms are used in calculations [see (16)]. For case (b), to examine the effect of the Raman term on the spectrum broadening, the Raman term is omitted [(21) and $f_R = 0$ in (16)]. For case (c), in addition, dispersion of the effective core area is omitted [$\partial_\omega(\ln g(\omega))|_{\omega_0} = 0$ in (12)], and for case (d), the SVEA is used [(21) and (16) with $f_R = 0$].

In Fig. 1, experimental spectra as well as calculated spectra are shown. It is seen that the agreement between the calculation with the equation including all the terms (a) and the experiment is good. When the Raman term is omitted (b), spectrum broadening at the short wavelength is larger in the calculations than in the experiment. This is because the optical energy is transferred to that at the longer wavelength by exciting the molecular vibrations when the Raman effect is present [1]. When the dispersion of the effective core area is omitted (c), spectral broadening at the long wavelength is larger in calculation than in experiment. This is because this effect is included as the additional steepening term in the calculation. When the steepening term is present, the trailing edge of the pulse becomes steep due to the intensity dependent group velocity [1]. This steep trailing edge generates large positive chirp from SPM. In this way, energy is transferred to the shorter wavelength when the steepening term is present. For the SVEA (d), spectrum broadening at the long wavelength is larger in the calculations than that in experiment. This is because no steepening term is included in the SVEA.

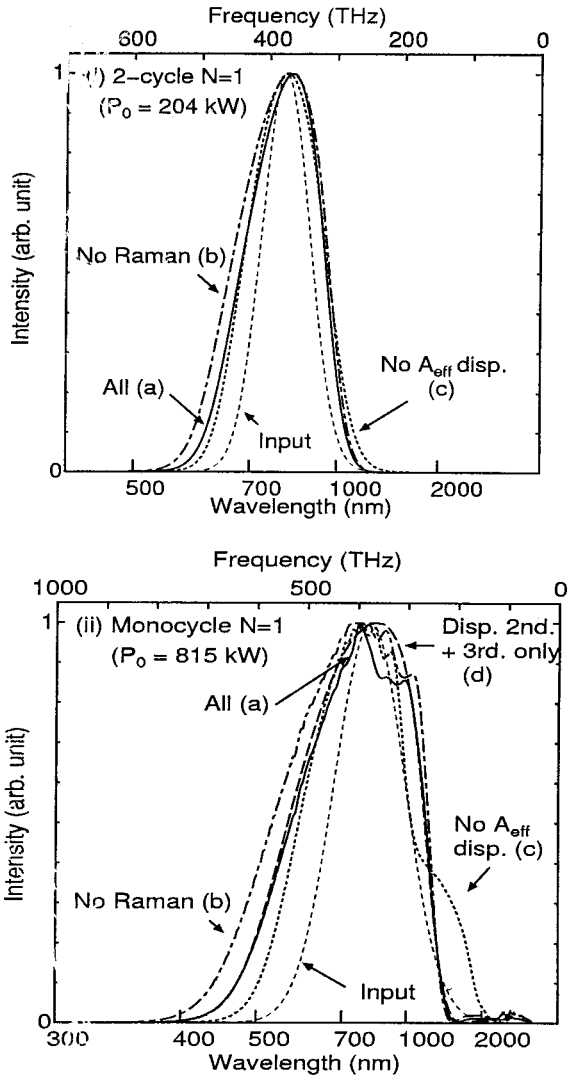


Fig. 2. Calculated spectra for: (i) 2-cycle pulses and (ii) monocycle, after propagating 2.5-mm-long fused-silica fiber. The soliton number N is 1 for both cases corresponding to 204-and 815-kW input powers for 2-cycle and monocycle cases, respectively. (a) All terms are included (solid line). (b) Without the Raman term (dotted-dashed line). (c) Without the effective core area dispersion (dotted line). (d) Only up to third-order dispersion terms in (a) are included (dashed line). Input spectra are shown by short dashed lines.

Also in this case, it was found that the spectrum including rigorous dispersion terms, and the spectrum including only up to third-order terms are almost identical. Thus, in this case, the approximation using up to the third-order term is sufficient.

B. Calculations of 2-Cycle and Monocycle Pulse SPM Cases

Calculations of spectra were performed for propagation of both 2-cycle pulse and a monocycle pulse. The fiber parameters are the same as in the previous subsection. Gaussian input pulses are used and the same soliton number of 1 is used in the calculations $(N = 1)$. The input pulse width and peak power are 5.32 fs and 204 kW for 2-cycle pulses and 2.66 fs and 815 kW for monocycle pulses, respectively.

Calculated spectra are shown in Fig. 2(i) for 2-cycle pulses. When the Raman term is not included (b), the spectrum intensity

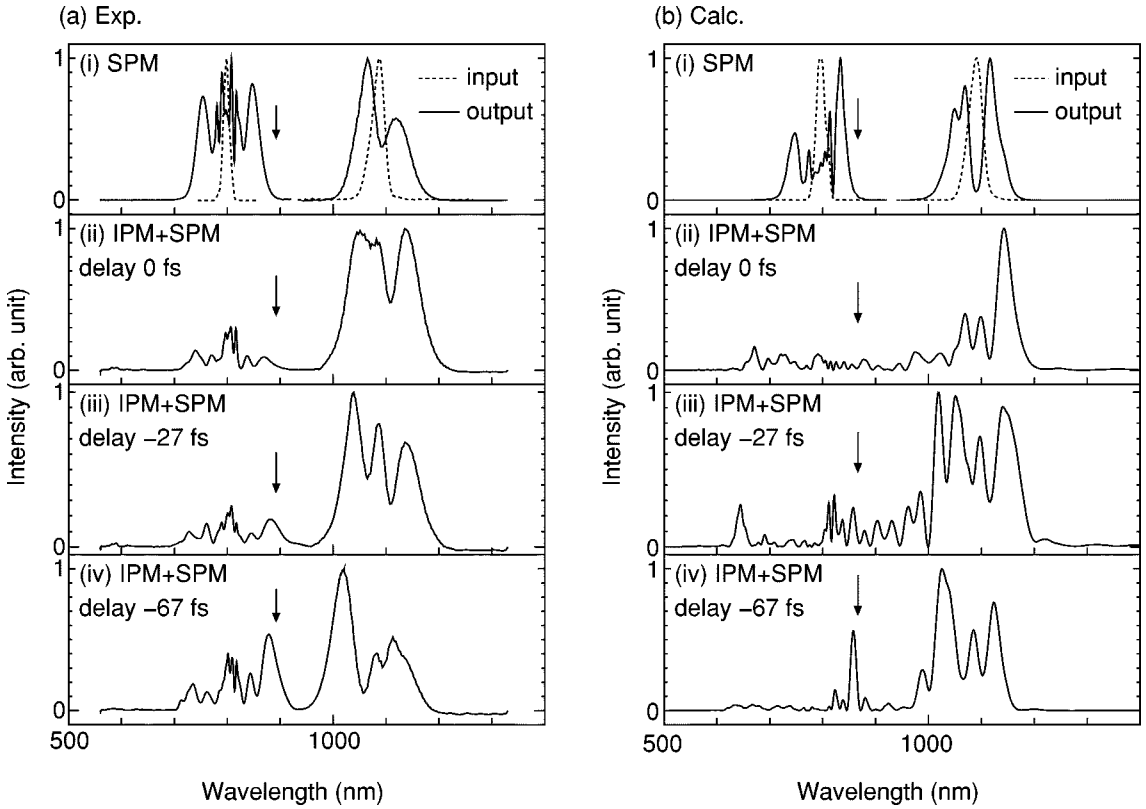


Fig. 3. (a) Experimental and (b) calculated spectra after the fundamental (center wavelength 797 nm, pulse width 79 fs, peak power 225 kW) and the idler (center wavelength 1087 nm, pulse width 75 fs, peak power 480 kW) pulses from the Ti:sapphire laser amplifier OPA system are propagated in a 3.5–mm-long fused-silica fiber. (i) Pulses propagated separately, with input spectra, are shown by dotted lines. (ii) Co-propagation of both pulses where the delay time of the fundamental pulse with respect to the idler pulse is set to be 0 fs. (iii) Co-propagation with delay time of -27 fs. (iv) Co-propagation with delay time of -67 fs.

at the short wavelength is larger than that with all terms (a). On the other hand, when dispersion of the effective core area is not included (c), the spectrum intensity at the long wavelength is larger than that with all terms.

The calculated spectra for the monocycle case are shown in Fig. 2(ii). Similar but more pronounced tendencies are observed when the Raman term is omitted (b) and dispersion of the effective core area is omitted (c), as compared with the calculations with all terms (a), like the 2-cycle pulse calculations. In this case, the additional calculation is carried out with the same terms as in (a) except that only up to third-order dispersion terms are included [$\hat{D}' = -\beta_0^{(2)}\partial_T^2/2 - i\beta_0^{(3)}\partial_T^3/6, \hat{D}_{\rm corr} = 0$ in (12)] is shown (d). There is a difference in spectra between this (d) and the one with all terms (a). Thus for this monocycle case, the inclusion of the dispersion terms only up to third-order terms is not enough. For the 2-cycle calculation, the same calculation is performed and no difference was found between these two spectra. Thus, for the calculation of the monocycle pulse, it is important to include more than the third-order term.

C. IPM+SPM Case

For the IPM experiments, the fundamental pulses (center wavelength 797 nm) and the idler pulses (center wavelength 1087 nm) from the Ti:sapphire amplifier system with the optical parametric amplifier (OPA) (BMI, alpha-1000 and comet 400s) was co-propagated in a 3.5-mm-long single-mode fiber (Newport F-SPV). The reflective objective was used to couple pulses in the fiber and the relative delay time between pulses was adjusted by an optical delay line with a micrometer and a position sensor. This delay was calibrated by observing the sum-frequency signal generated by both pulses using a 10 μm-thick β barium borate (BBO) crystal. In this experiment, both input pulses were evaluated by a second-harmonic, frequency-resolved optical gating (SH FROG) apparatus [16]. The measured pulse widths were 75 and 79 fs for the fundamental and the idler waves, respectively. The spectra when each pulse was propagated separately (i) and when both pulses were co-propagated with one of three different delay times of the fundamental pulse with respect to the idler pulse (0 fs (ii), -27 fs (iii) and -67 fs (iv)) are shown in Fig. 3(a). The effective core area $A_{\rm eff}$ and its dispersion $-\omega_0\partial_\omega(\ln A_{\rm eff}(\omega))|_{\omega_0}$ are included alike in the SPM case, which are $2.05(4.92)\pi a^2$ and $2.06(3.80)$ for the fundamental (idler) waves, respectively. The cross overlap integral is given as $O(\omega_{01},\omega_{02}) = 3.30$ πa^2 and its dispersions $-\omega\partial_\omega(\ln O(\omega,\omega_{03} - j))_{\omega 0j}$ are calculated to be 0.837 and 2.19 for fundamental $(j = 1)$ and idler $(j = 2)$ waves, respectively. Due to the difficulty of separating the propagated output pulse energy from the pulse energy propagating in the cladding, the input power for each pulse was estimated by fitting of the SPM measurements and was determined to be 225 (480) kW for the fundamental (idler) waves. The calculated spectra from (17) are compared with the experimental ones in Fig. 3(b). It is shown in both cases of the experiment and the calculation that, when these pulses are propagated separately (i), there is no intensity between 880–970 nm. When both pulses are co-propagated (ii)–(iv), the spectra

for the fundamental wave and the idler wave are connected by IPM. The intensity of the middle position (indicated by arrows in Fig. 3) is the largest when the delay time is -67 fs compared with that when the delay time is 0 fs. The propagation time difference between these two pulses for a 3.5-mm-long fiber is 58.6 fs. Thus, when the delay time is -67 fs, both pulses overlap near the fiber exit end. For the capillary fiber IPM using the fundamental and the second-harmonic pulses, we have analytically [6] and experimentally shown [7] that the spectrum overlapping becomes largest when both pulses meet near the fiber exit end. The present results indicate that a similar tendency holds for the fused-silica fiber. It is observed that the delay time dependence of the spectra between the experiment and theory agree qualitatively.

VIII. Conclusion

The nonlinear pulse propagation equations for a single pulse propagation and for co-propagation of two pulses in a fiber that include rigorous linear dispersions, the Raman effect and the dispersion of the effective core area that can be used for pulses in the single-cycle regime, were derived. These were used in the calculations for SPM spectral broadening and SPM and IPM spectral broadening in single-mode fused-silica fiber and were compared with the experimental results. For the SPM case with the 4.5-cycle pulse, calculations using the newly derived equation gave spectra that agreed well with the experimental spectrum. The effects of omitting the Raman term and the dispersion of the effective core area were investigated. It was found that when the Raman term was omitted, the relative intensity at the shorter wavelength became larger and when the dispersion of the effective core area was omitted, the relative intensity at the longer wavelength became larger. The calculations for 2-cycle and monocycle pulses were performed and it was shown that the inclusion of up to the third-order dispersion terms was enough for the 2-cycle pulse but not enough for the monocycle pulse. The co-propagation of the fundamental and the idler waves from the Ti:sapphire OPA system was experimentally performed and the spectra from IPM as well as SPM as a function of delay time were measured and compared with calculated spectra. The dependence of the spectra untime delay was shown to be similar to the capillary fiber case and the calculated spectra agreed qualitatively with the experimental spectra.

References

[1] G. P. Agrawal, *Nonlinear Fiber Optics*, 2nd ed. San Diego, CA: Academic, 1989.

[2] E. A. J. Marcatili and R. A. Schmeltzer, "Hollow metallic and dielectric waveguides for long distance optical transmission and lasers," *Bell Sys. Tech. J.*, vol. 43, pp. 1783–1809, 1960.

[3] M. Yamashita, H. Sone, and R. Morita, "Proposal for generation of a coherent pulse ultra-broadened from near-infrared to near-ultraviolet and its monocyclization," *Jpn. J. Appl. Phys.*, vol. 35, pp. L1194–L1197, 1996.

[4] M. Yamashita, H. Sone, R. Morita, and H. Shigekawa, "Generation of monocycle-like optical pulses using induced-phase modulation between two-color femtosecond pulses with carrier-phase locking," *IEEE J. Quantum Electron.*, vol. 34, pp. 2145–2149, 1998.

[5] L. Xu, N. Karasawa, N. Nakagawa, R. Morita, H. Shigekawa, and M. Yamashita, "Experimental generation of an ultra-broad spectrum based on induced-phase modulation in a single-mode glass fiber," *Opt. Commun.*, vol. 162, pp. 256–260, 1999.

[6] N. Karasawa, R. Morita, L. Xu, H. Shigekawa, and M. Yamashita, "Theory of ultrabroadband optical pulse generation by induced phase modulation in a gas-filled hollow waveguide," *J. Opt. Soc. Amer. B*, vol. 16, pp. 662–668, 1999.

[7] N. Karasawa, R. Morita, H. Shigekawa, and M. Yamashita, "Generation of intense ultrabroadband optical pulses by induced phase modulation in an argon-filled single-mode hollow waveguide," *Opt. Lett.*, vol. 25, pp. 183–185, 2000.

[8] R. H. Stolen, J. P. Gordon, W. J. Tomlinson, and H. A. Haus, "Raman response function of silica-core fibers," *J. Opt. Soc. Amer. B*, vol. 6, pp. 1159–1166, 1989.

[9] R. H. Stolen and W. J. Tomlinson, "Effect of the Raman part of the nonlinear refractive index on propagation of ultrashort optical pulses in fibers," *J. Opt. Soc. Amer. B*, vol. 9, pp. 565–573, 1992.

[10] T. Brabec and F. Krausz, "Nonlinear optical pulse propagation in the single-cycle regime," *Phys. Rev. Lett.*, vol. 78, pp. 3282–3285, 1997.

[11] K. J. Blow and D. Wood, "Theoretical description of transient stimulated Raman scattering in optical fibers," *IEEE J. Quantum Electron.*, vol. 25, pp. 2665–2673, 1989.

[12] P. V. Mamyshev and S. V. Chernikov, "Ultrashort-pulse propagation in optical fibers," *Opt. Lett.*, vol. 15, pp. 1076–1078, 1990.

[13] G. Boyer, "High-power femtosecond-pulse reshaping near the zero-dispersion wavelength of an optical fiber," *Opt. Lett.*, vol. 24, pp. 945–948, 1999.

[14] I. H. Malitson, "Interspecimen comparison of the refractive index of fused silica," *J. Opt. Soc. Amer.*, vol. 35, pp. 1205–1209, 1965.

[15] A. J. Taylor, G. Rodriguez, and T. S. Clement, "Determination of n_2 by direct measurement of the optical phase," *Opt. Lett.*, vol. 21, pp. 1812–1814, 1996.

[16] D. J. Kane and R. Trebino, "Characterization of arbitrary femtosecond pulses using frequency-resolved optical gating," *IEEE J. Quantum Electron.*, vol. 29, pp. 571–579, 1993.

Naoki Karasawa, photograph and biography not available at the time of publication.

Shinki Nakamura, photograph and biography not available at the time of publication.

Naoya Nakagawa, photograph and biography not available at the time of publication.

Masato Shibata, photograph and biography not available at the time of publication.

Ryuji Morita, photograph and biography not available at the time of publication.

Hidemi Shigekawa, photograph and biography not available at the time of publication.

Mikio Yamashita, photograph and biography not available at the time of publication.